Kilowatt-Scale Large Air-Gap Multi-Modular Capacitive Wireless Power Transfer System for Electric Vehicle Charging

Brandon Regensburger, Sreyam Sinha, Ashish Kumar, Jason Vance, Zoya Popović and Khurram K. Afridi
Department of Electrical, Computer, and Energy Engineering
University of Colorado Boulder
Boulder, USA
brandon.regensburger@colorado.edu; khurram.afridi@colorado.edu

***Abstract*—This paper introduces a high-performance kilowatt-scale large air-gap multi-modular capacitive wireless power transfer (WPT) system for electric vehicle (EV) charging. This multi-modular system achieves high power transfer while maintaining fringing electric fields within prescribed safety limits. The fringing fields are reduced using near-field phased-array field-focusing techniques, wherein the adjacent modules of the multi-modular system are out-phased with respect to one another. The inter-module interactions in this multi-modular system are modeled, and an approach to eliminate these interactions in a practical EV charging environment is proposed. A prototype 1.2-kW 6.78-MHz 12-cm air-gap multi-modular capacitive WPT system comprising two 600-W modules is designed, built and tested. This prototype system achieves 21.2 kW/m^2 power transfer density and a peak efficiency of 89.8%. This multi-modular system also achieves a fringing field reduction of 50% compared to its individual modules.**

Keywords—wireless power transfer; capacitive wireless power transfer; large air-gap; electric vehicle; high efficiency; high power transfer density; matching networks; high frequency; near-field phased array field focusing

I. INTRODUCTION

Market penetration of electric vehicles (EVs) remains low, with EV sales in the US accounting for under 1% of total vehicle sales [1]. Major challenges in widespread EV adoption are high cost, limited range and long charging times, due to limitations in battery technology. An effective approach to overcome these challenges is to substantially reduce on-board energy storage and instead utilize dynamic (in-motion) wireless power transfer (WPT) to deliver energy to the vehicle from the roadway. WPT for EVs can be achieved either using magnetic fields between inductively coupled coils, or using electric fields between capacitively coupled plates. Inductive WPT systems require ferrites for magnetic flux guidance; these ferrites are expensive, heavy, fragile, and necessitate a low operating frequency to limit core losses [2], resulting in relatively large system size. In contrast, capacitive WPT systems do not require ferrites and can operate at high frequencies, allowing these systems to be less expensive, more efficient, lighter, more compact and easier to embed in the roadway. Large air-gap capacitive WPT for EV charging applications has been recently examined in [3]-[16]. Owing to the large air-gap and the limited area available under the vehicle chassis (which together result in a very small coupling capacitance), designing high-power high-efficiency capacitive WPT systems for EV charging is very challenging. Furthermore, in practical implementations of these systems, it is imperative to maintain fringing electric fields below the prescribed safety limits [17].

This paper introduces a high-performance large air-gap multi-modular capacitive WPT system suitable for EV charging. This system achieves high power transfer at high efficiency using an innovative design approach that involves the modeling and mitigation of inter-module interactions, and maintains fringing electric fields within safety limits using near-field phased-array field-focusing techniques [3]. A prototype 1.2-kW 6.78-MHz 12-cm air-gap multi-modular capacitive WPT system comprising two 600-W modules, each utilizing 12.25-cm × 12.25-cm capacitive coupling plates has been designed, built and tested. The prototype system transfers up to 1275 W, achieving a power transfer density of 21.2 kW/m^2 and a peak efficiency of 89.8%. The two modules of the prototype system are phased relative to one another by 180°, resulting in a 50% reduction in the measured fringing electric fields compared to a single 600-W module.

The remainder of this paper is organized as follows: Section II introduces the architecture of the multi-modular capacitive WPT system. Section III presents an approach to model and mitigate the inter-module interactions in this system. Experimental results from the prototype multi-modular capacitive WPT system are presented in Section IV. Finally, Section V summarizes and concludes the paper.

II. MULTI-MODULAR CAPACITIVE WPT ARCHITECTURE

The architecture of a large air-gap multi-modular capacitive WPT system for EV charging is shown in Fig. 1. Wireless power transfer in the individual modules of this system is accomplished using two pairs of conducting plates, one pair embedded in the vehicle chassis, and the other embedded in the road. Each module comprises a high-frequency inverter and rectifier, and two matching networks that enable effective power transfer by providing voltage and/or current gain and reactive compensation. The inverter converts the dc voltage at the input of the module to a high-frequency ac voltage. This ac voltage is

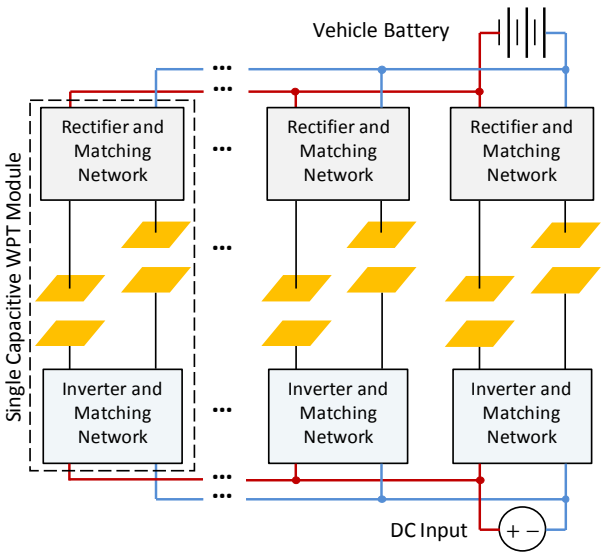

Fig. 1: Architecture of a multi-modular capacitive WPT system. Each module comprises two pairs of coupling plates, a high-frequency inverter and rectifier, and matching networks that provide gain and reactive compensation.

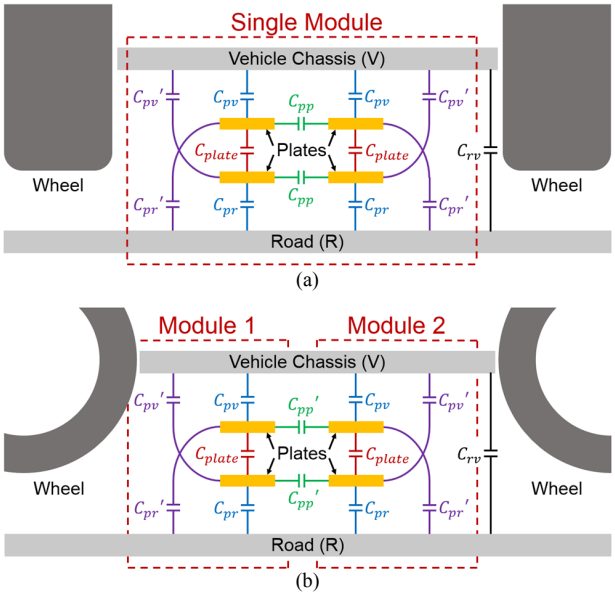

Fig. 2: The various capacitances present in a two-module capacitive WPT system in a practical EV charging environment: (a) viewed from the front/rear of the vehicle, and (b) viewed from the side of the vehicle.

stepped up by the matching network, creating a high voltage at the road side of the coupling plates. On the vehicle side of the coupling plates, the second matching network steps the current up (and the voltage down) to the level required to charge the vehicle battery, and a rectifier then converts the ac current (and voltage) to dc. Additionally, the two matching networks together compensate for the capacitive reactance of the coupling plates. The inverters of the adjacent modules of this multi-modular system are operated with a phase-shift relative to one another. By appropriately selecting this phase-shift, the fringing electric fields generated by adjacent modules can be canceled, ensuring that the field strengths in areas of concern, such as the regions beyond the vehicle chassis, are maintained below prescribed safety limits.

III. Modeling and Mitigation of Inter-Module Interactions

The couplers in each module of the multi-modular capacitive WPT system of Fig. 1 would ideally be equivalent to two coupling capacitances. However, several additional parasitic capacitances exist in a practical EV charging scenario, as shown for a two-module capacitive WPT system in Fig. 2. Figure 2(a) shows these capacitances as viewed from the front/rear of the vehicle, and Fig. 2(b) provides a side view. These parasitic capacitances create undesirable intra-module and inter-module interactions, which can severely degrade power transfer and efficiency, particularly when operating at high (multi-MHz) frequencies. Therefore, to achieve high power transfer levels and high efficiencies, it is important to identify ways to decouple the individual modules from one another, and absorb the parasitic capacitances within each module. Such an approach is discussed below.

A circuit schematic of the two-module capacitive WPT system incorporating the parasitic capacitances, and utilizing L-section matching networks for gain and compensation, is shown in Fig. 3(a). The two modules have identical designs, and their inverters are operated at a relative phase-shift of 180° to maximize fringing field cancelation. Using phasor analysis under this 180°-phased condition, it can be shown that the effect of the inter-module plate-to-plate capacitances (labeled as $C_{pp}{}'$ in Fig. 3(a)) can be modeled using capacitances of the same magnitude appearing inside the individual modules, as shown in Fig. 3(b); hence, partially decoupling the two modules. This can be understood as follows. Since the two modules are phased apart by 180°, the node P_2 in the top module is at the same voltage as the node P_5 in the bottom module, both relative to the inverter ground. Therefore, the current that flows from node P_1 in the top module to node P_5 in the bottom module through the inter-module capacitance $C_{pp}{}'$ can be equivalently modeled by the same current flowing between nodes P_1 and P_2 of the top module, through a capacitance of the same value $C_{pp}{}'$. Similarly, the other inter-module capacitance $C_{pp}{}'$ between nodes P_2 and P_6 can be modeled by a capacitance of the same value between nodes P_5 and P_6 of the bottom module. A similar modeling approach applies to the vehicle-side inter-module plate-to-plate capacitances. The two modules in Fig. 3(b) are still coupled to one another through the plate-to-road capacitances, C_{pr} and $C_{pr}{}'$, and the plate-to-vehicle capacitances, C_{pv} and $C_{pv}{}'$. The effect of these capacitances is mitigated by enforcing circuit symmetry, wherein the inductors of the L-section matching networks in both modules (L_1 and L_2) are split into two equal halves, one in the forward and the other in the return path, as also shown in Fig. 3(b). This ensures that the voltages at the two same-side coupling plates in each module (for instance, nodes P_1 and P_2 in Fig. 3(b)), relative to the road and vehicle chassis (nodes R and V in Fig. 3(b), respectively), are equal in magnitude and opposite in phase. As a result, the current that flows through one pair of coupling plates in a module is equal to

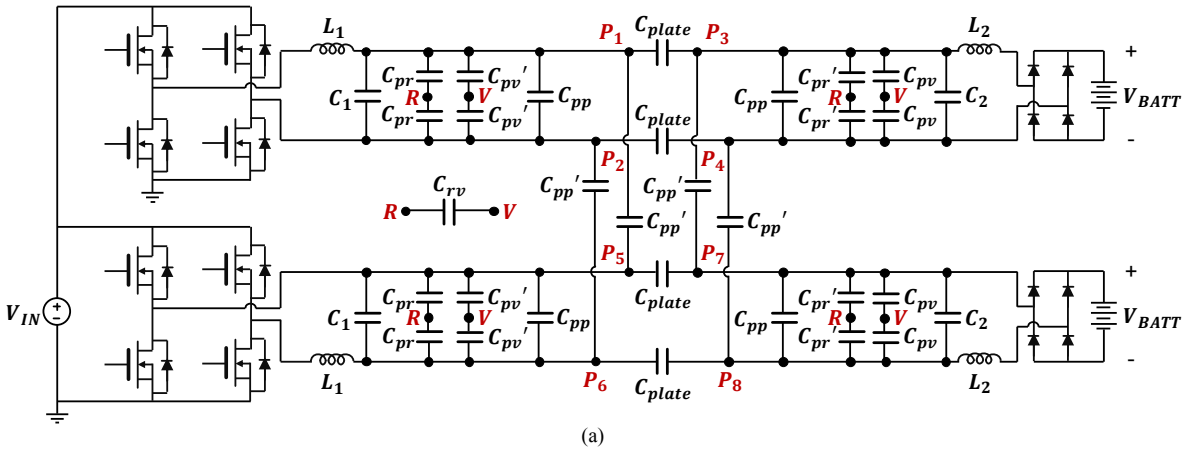

(a)

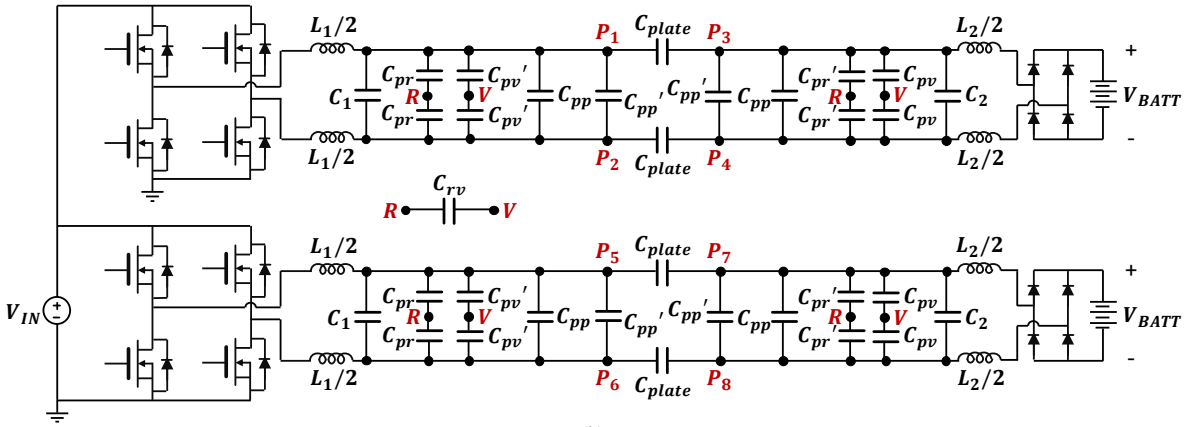

(b)

Fig. 3: Circuit schematic of a two-module capacitive WPT system: (a) with the inter-module parasitic capacitances shown based on their physical manifestation, and (b) with the two modules effectively decoupled by: (1) an equivalent model for the inter-module plate-to-plate capacitances (C_{pp}'), valid when the modules are operated 180° out of phase, allowing the C_{pp}'s to be absorbed within the individual modules, and (2) by eliminating the effect of the other inter-module capacitances through symmetrically split inductor design.

the return current through the other pair in the same module; hence, the two modules appear fully decoupled. Furthermore, in this symmetrically-designed decoupled system, the parasitic capacitances can be used to fully realize the matching network capacitors of the individual modules, as shown in Fig. 4, where $C_{ps1}\left(= C_{pp} + C_{pp}' + \frac{C_{pr}}{2} + \frac{C_{pv}'}{2}\right)$ and $C_{ps2}\left(= C_{pp} + C_{pp}' + \frac{C_{pv}}{2} + \frac{C_{pr}'}{2}\right)$ are utilized as the required matching network capacitances. This eliminates the need for discrete capacitors that are prone to dielectric breakdown, and enables the parasitic

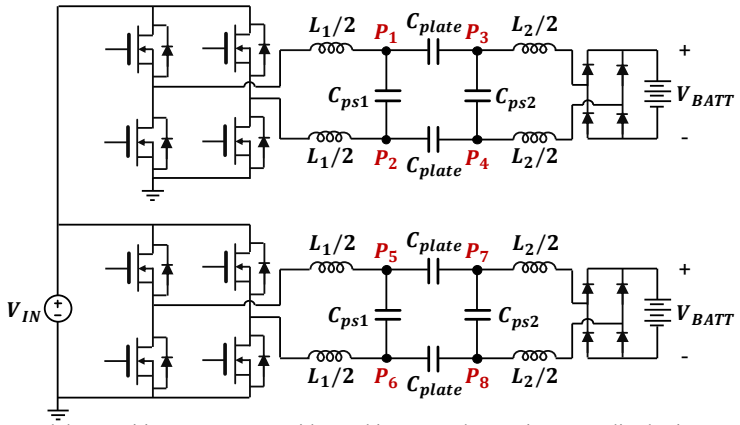

Fig. 4: Circuit schematic of the two-module capacitive WPT system with matching network capacitances realized using parasitic capacitances.

capacitances to enhance, rather than degrade, power transfer. Note that this approach to modeling and mitigating inter-module interactions and absorbing parasitic capacitances into the matching networks of individual modules can be extended to a multi-modular system comprising a higher number of modules.

The L-section matching networks of the capacitive WPT system of Fig. 4 provide voltage and/or current gain, and compensate for the reactance of the coupling plates. A framework for optimally designing the matching networks of a single-module capacitive WPT system was presented in [7], and guidelines for ensuring that the inductors of these matching networks have sufficiently high quality factors and self resonant frequencies were presented in [8]. The work in [12] leverages the framework and guidelines of [7] and [8] to develop a comprehensive design methodology for designing the matching networks of a single-module capacitive WPT system. Since the modules of the multi-modular system presented here are effectively decoupled using the above-described approach, the methodology of [12] is utilized to design the matching networks of each module.

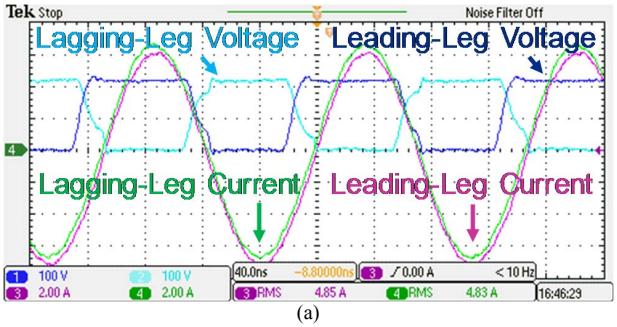

(a)

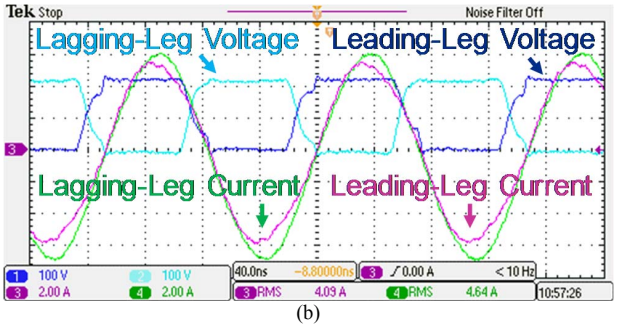

(b)

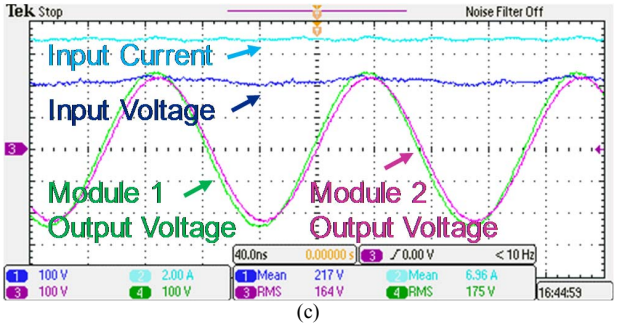

(c)

Fig. 6: Measured waveforms of the prototype multi-module capacitive WPT system operating at 1275 W: (a) inverter switch node voltages and currents of module 1, (b) inverter switch node voltages and currents of module 2, and (c) system input voltage and current, and the output voltages of the two modules.

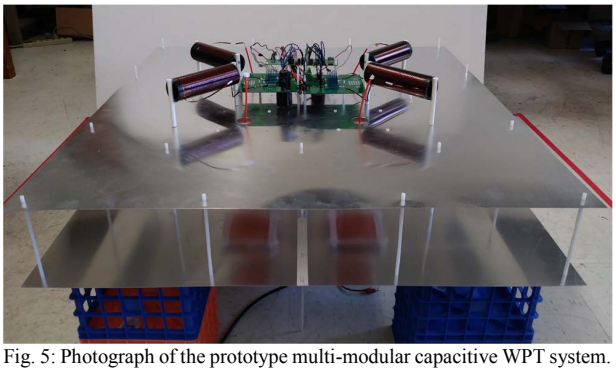

Fig. 5: Photograph of the prototype multi-modular capacitive WPT system.

IV. Prototype Design and Experimental Results

A prototype 1.2-kW 6.78-MHz 12-cm air-gap multi-modular capacitive WPT system utilizing 12.25-cm × 12.25-cm coupling plates is designed, built and tested. This prototype comprises two identical 600-W modules similar to those shown in Fig. 3, with the one difference being that the rectifier and battery are emulated by resistors. A photograph of the prototype system is shown in Fig. 5. The aluminum sheets visible in Fig. 5 are used to mimic the road and the vehicle chassis, and the vertical distance between these sheets and the coupling plates is controlled to realize the desired matching network capacitances. The matching network inductors are realized as single-layer air-core solenoids. Values of the coupling capacitance, the matching network inductances and capacitances, and the load resistance of the prototype system are provided in Table I. The inverters of the prototype system are constructed using 650-V 22.5-A GaN Systems GS66506T enhancement-mode GaN transistors. Measured waveforms of the prototype multi-modular system while transferring 1275 W are shown in Fig. 6. It can be seen

TABLE I. Select Circuit Parameters of the Prototype Capacitive WPT System

C_{plate} [pF]	L_1 [µH]	L_2 [µH]	C_{ps1} [pF]	C_{ps2} [pF]	R_{load} [Ω]
0.88	53	53	9.58	9.58	45

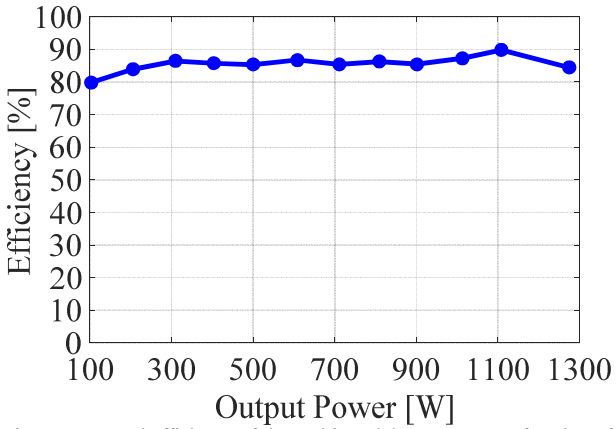

Fig. 7: Measured efficiency of the multi-modular system as a function of its output power.

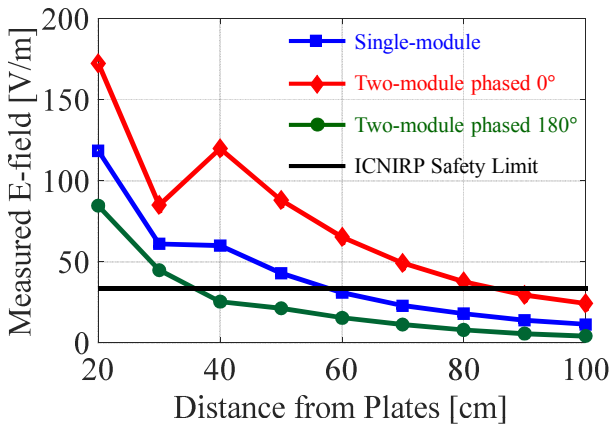

Fig. 8: Measured fringing electric field magnitude as a function of distance from the coupling plates, for three different configurations of the capacitive WPT system. The dip that can be observed at a distance of 30 cm from the coupling plates is due to edge effects: at this distance, the electric field probe is directly underneath the edge of the aluminum sheets that mimic the vehicle chassis and the road.

from Figs. 6(a) and 6(b) that the inverters of both modules operate with zero-voltage switching (ZVS). The measured efficiency of the multi-modular system is shown as a function of its output power in Fig. 7. As can be seen, the prototype system maintains a flat efficiency across the entire output power range, and achieves a peak efficiency of 89.8%. The 1.2-kW prototype achieves a power transfer density of 21.2 kW/m^2, which, to the authors' best knowledge, is more than five times higher than the state-of-the-art in capacitive WPT systems, and comparable to inductive WPT systems for EV charging.

The fringing electric fields of the 1.2-kW multi-modular system have also been measured. For these measurements, the system was operated in three configurations: first, with only one module active and delivering 500 W; second, with both modules active, delivering a total of 1 kW, and operating at 0° phase relative to one another; and third, with both modules active, again delivering 1 kW, but operating at 180° phase relative to one another. A plot of the measured fringing electric field magnitude as a function of distance from the edge of the coupling plates for all three configurations is shown in Fig. 9. As can be seen from Fig. 8, the fringing fields in the 0°-phased 1-kW multi-modular configuration (shown in red) are significantly higher than those in the 500-W single-module configuration (shown in blue). However, the fringing fields in the 180°-phased 1-kW multi-modular configuration (shown in green) are substantially lower than even the 500-W single-module configuration, with an average reduction of nearly 50%. This reduction in fringing electric fields enables the 180°-phased 1-kW multi-modular system to meet the 33.4 V/m ICNIRP electric field safety limit [17], shown in black in Fig. 9, at a distance of 36 cm away from the edge of the coupling plates, as compared to a distance of 58 cm for the 500-W single module and 85 cm for the 0°-phased 1-kW system.

V. Conclusions

This paper introduces a high-performance kilowatt-scale large air-gap multi-modular capacitive WPT system for EV charging. This multi-modular system achieves high power transfer levels while reducing fringing electric fields using near-field phased-array field-focusing techniques. The inter-module interactions in this multi-modular system are modeled, and an approach to mitigate these interactions in a practical EV charging environment is introduced. A prototype 1.2-kW 6.78-MHz 12-cm air-gap multi-modular capacitive WPT system comprising two 600-W modules is designed, built and tested. This prototype system achieves a power transfer density of 21.2 kW/m^2 and a peak efficiency of 89.8%. The prototype multi-modular system also achieves a fringing field reduction of 50% compared to its individual modules.

Acknowledgment

The authors would like to acknowledge the Advanced Research Projects Agency – Energy (ARPA-E) for financially supporting this work under Award Number DE-AR0000618.

References

[1] The Electric Vehicle World Sales Database, "Plug-in Vehicle Sales for Q2 and Year to Date", 2017. [Online]. Available: www.ev-volumes.com/country/usa/. [Accessed: November 20, 2017].

[2] G.A. Covic and J.T. Boys, "Modern Trends in Inductive Power Transfer for Transportation Applications," *IEEE Journal of Emerging and Selected Topics in Power Electronics*, vol. 1, no. 1, pp. 28-41, March 2013.

[3] A. Kumar, S. Pervaiz, C.K. Chang, S. Korhummel, Z. Popovic and K.K. Afridi, "Investigation of Power Transfer Density Enhancement in Large Air-Gap Capacitive Wireless Power Transfer Systems," *Proceedings of the IEEE Wireless Power Transfer Conference (WPTC)*, Boulder, CO, May 2015.

[4] F. Lu, H. Zhang, H. Hofmann and C. Mi, "A Double-Sided LCLC-Compensated Capacitive Power Transfer System for Electric Vehicle Charging," *IEEE Transactions on Power Electronics*, vol. 30, no. 11, pp. 6011-6014, November 2015.

[5] F. Lu, H. Zhang, H. Hofmann and C. Mi, "A CLLC-compensated high power and large air-gap capacitive power transfer system for electric vehicle charging applications," *Proceedings of the IEEE Applied Power Electronics Conference and Exposition (APEC)*, Long Beach, CA, March 2016.

[6] I. Ramos, K.K. Afridi, J. A. Estrada and Z. Popović, "Near-Field Capacitive Wireless Power Transfer Array with External Field Cancellation," *Proceedings of the IEEE Wireless Power Transfer Conference (WPTC)*, Aveiro, Portugal, May 2016.

[7] S. Sinha, A. Kumar, S. Pervaiz, B. Regensburger and K.K. Afridi, "Design of Efficient Matching Networks for Capacitive Wireless Power Transfer Systems," *Proceedings of the IEEE Workshop on Control and Modeling for Power Electronics (COMPEL)*, Trondheim, Norway, June 2016.

[8] K. Doubleday, A. Kumar, S. Sinha, B. Regensburger, S. Pervaiz and K.K. Afridi, "Design Tradeoffs in a Multi-Modular Capacitive Wireless Power Transfer System," *Proceedings of the IEEE PELS Workshop on Emerging Technologies: Wireless Power Transfer (WoW)*, Knoxville, TN, October 2016.

[9] F. Lu, H. Zhang, H. Hofmann, Y. Mei and C. Mi, "A Dynamic Capacitive Power Transfer System with Reduced Power Pulsation," *Proceedings of the IEEE PELS Workshop on Emerging Technologies: Wireless Power Transfer (WoW)*, Knoxville, TN, October 2016.

[10] F. Lu, H. Zhang, H. Hofmann and C. Mi, "An Inductive and Capacitive Combined Wireless Power Transfer System with LC-Compensated Topology," *IEEE Transactions on Power Electronics*, vol. 31, no. 12, pp. 8471-8482, December 2016.

[11] H. Zhang, F. Lu, H. Hofmann, W. Liu and C.C. Mi, "A Four-Plate Compact Capacitive Coupler Design and LCL-Compensated Topology for Capacitive Power Transfer in Electric Vehicle Charging Application," *IEEE Transactions on Power Electronics*, vol. 31, no. 12, pp. 8541-8551, December 2016.

[12] B. Regensburger, A. Kumar, S. Sinha, K. Doubleday, S. Pervaiz, Z. Popović, K.K. Afridi, "High-Performance Large Air-Gap Capacitive Wireless Power Transfer System for Electric Vehicle Charging," *Proceedings of the IEEE Transportation Electrification Conference and Expo (ITEC)*, Chicago, IL, June 2017.

[13] K. Doubleday, A. Kumar, B. Regensburger, S. Pervaiz, S. Sinha, Z. Popovic and K.K. Afridi, "Multi-Objective Optimization of Capacitive Wireless Power Transfer Systems for Electric Vehicle Charging," *Proceedings of the IEEE Workshop on Control and Modeling for Power Electronics (COMPEL)*, Stanford, CA, July 2017.

[14] S. Sinha, B. Regensburger, K. Doubleday, A. Kumar, S. Pervaiz and K.K. Afridi, "High-Power-Transfer-Density Capacitive Wireless Power Transfer System for Electric Vehicle Charging," *Proceedings of the IEEE Energy Conversion Congress and Exposition (ECCE)*, Cincinnati, OH, October 2017.

[15] J. Estrada, S. Sinha, B. Regensburger, K.K. Afridi and Z. Popovic, "Capacitive Wireless Powering for Electric Vehicles with Near-Field Phased Arrays," *Proceedings of the European Microwave Conference*, Nuremburg, Germany, October 2017.

[16] S. Sinha, A. Kumar, B. Regensburger, and K.K. Afridi, "A Very-High-Power-Transfer-Density GaN-Based Capacitive Wireless Power Transfer System," *Proceedings of the IEEE Workshop on Wide Bandgap Power Devices and Applications (WiPDA)*, Albuquerque, NM, October/November 2017.

[17] International Commission on Non-Ionizing Radiation Protection, "ICNIRP Guidelines for Limiting Exposure to Time-Varying Electric, Magnetic and Electromagnetic Fields (1 Hz to 100 kHz)," *Health Physics*, vol. 99, no. 6, pp. 818–836, December 2010.